Original Study

Yong-Joo Jwa*, Seonbok Yi, Mi-Eun Jin, Ga-Hyun Hwang

Two Contrasting Provenances of Prehistoric Obsidian Artifacts in South Korea: Mineralogical and Geochemical Characteristics

https://doi.org/10.1515/opar-2019-0008
Received March 31, 2018; accepted December 10, 2018

Abstract: Two provenances – Mount Baekdusan near Sino-Korean border and Kyushu of southwest Japan – are well known for Korean prehistoric obsidian artifacts. We examined the mineralogical and geochemical characteristics of the Baekdusan obsidians and the Kyushu obsidians. Though obsidians are of glassy material, microlites are easily found in the host matrix. Fe-oxides are the most abundant microlite phase, with a lesser amount of clinopyroxene, feldspar, and biotite. It is notable that the texture and chemical composition of the microlites in the Baekdusan obsidians are quite different from those in the Kyushu obsidians. Clinopyroxene in the Baekdusan obsidians occurs as oikocryst enclosing smaller Fe-oxides, and has the composition of hedenbergite to augite. On the other hand, clinopyroxene in the Kyushu obsidians is compositionally of clinoferrosilite, and shows intergrowth and/or overgrowth textures with Fe-oxides. Feldspar microlites in the Baekdusan obsidians are generally of sanidine to anorthoclase, whereas those in the Kyushu obsidians of oligoclase. Biotite microlites are often found in the Kyushu obsidians, but absent in the Baekdusan obsidians. Also, there exist prominent geochemical contrasts between the Baekdusan obsidians and the Kyushu obsidians. At the similar SiO2 range of 74 to 78 wt.% the host glasses of the Baekdusan obsidians have higher contents of TiO2, total FeO, K2O, Nb, Hf, Zr, Ta, Y and rare earth elements (REEs) than those of the Kyushu obsidians. The overall mineralogical and geochemical contrasts for the Baekdusan and Kyushu obsidians seem to reflect different parental magma composition and crystallization environment. This distinction can be used to establish the provenance of the obsidian artifacts from the prehistoric sites in the Korean Peninsula as well as contiguous areas such as China, Japan, and Russia.

Keywords: provenance, Baekdusan, Kyushu, obsidian, microlite, morphology, matrix, geochemistry

Article note: This article is a part of Topical Issue on Scientific Studies of Obsidian Sources and Trade, edited by Robert H. Tykot, Maria Clara Martinelli, Andrea Vianello

***Corresponding author: Yong-Joo Jwa**, Department of Geology and Research Institute of Natural Sciences, Gyeongsang National University, Jinju 52828, Korea, E-mail: jwayj@gnu.ac.kr
Mi-Eun Jin, Ga-Hyun Hwang, Department of Geology and Research Institute of Natural Sciences, Gyeongsang National University, Jinju 52828, Korea
Seonbok Yi, Department of Archaeology, Seoul National University, Seoul 08826, Korea
Mi-Eun Jin, Neutron Science Division, Korea Atomic Energy Research Institute, Daejeon 34057, Korea
Ga-Hyun Hwang, Restoration Technology Division, National Research Institute of Cultural Heritage, Daejeon 34122, Korea

1 Introduction

In South Korea, obsidian artifacts are known at many prehistoric sites, and all of the sites are open-air localities dated between c. 25–30 ka and 5–6 ka. Although some of the Pleistocene localities are thought to have features related to human habitation, they basically represent loose accumulations of artifacts over time in fluvio-colluvial sediments. Association between obsidian artifacts and such features is more pronounced for the Neolithic, although they are not reported in the context of tool-making or use. In Korea, obsidian is a rather rare rock to be found: a limited amount of obsidian is known to occur in Meso- to Cenozoic volcanic fields in South Korea but its quality and quantity are not adequate for producing artifacts. The only known source of obsidian material fine enough to make prehistoric tools is Mt. Baekdusan (also known as Paektusan and Changbaishan) volcanic field close to the Sino-Korean border. On the other hand, the Kyushu volcanic field in southwestern Japan is well known for many obsidian sources.

Regarding the provenance of the obsidian artifacts, there currently are a couple of contrasting opinions among the researchers. One is that they are mostly from the Baekdusan area (the obsidian artifacts from Hahwagyeri, Hopyeongdong, Jangheungri, Sangmuryongri, Samri, and Suyanggae sites in Fig. 1; Sohn, 1989; Kuzmin, 2004; Kim et al., 2007), and the other is that there are included other than Baekdusan materials whose sources must be delineated (Gigok, Sangsari, Sinbuk, and Wolseongdong sites in Fig. 1; Cho et al., 2006; Jang et al., 2007; Cho & Choi, 2010, 2012). Recently laser-ablation ICP-MS (LA-ICP-MS) analyses were conducted for the obsidian artifacts from the Sinbuk and Wolsoengdong sites (Lee & Kim, 2015; Chang & Kim, 2018). Multi-elemental analyses using these new geochemical data suggest that the Sinbuk obsidians represent a bimodal source from the Baekdusan and Kyusu (Lee & Kim, 2015), and that the Wolseongdong obsidians originated from a single Baekdusan source (Chang & Kim, 2018). At the same time, it is noted that obsidian artifacts from the southern part of South Korea demonstrate genetic similarity to the Kyushu obsidians (Dongsamdong, Tongyeong, and Yeosu sites in Fig. 1; Cho et al., 2006; Jang et al., 2007; Kim et al., 2007). It is, therefore, important to understand the compositional contrast between the Baekdusan and Kyushu obsidians in clarifying the provenance of the Korean obsidian artifacts.

Obsidian is rhyolitic glass in geological nomenclature (Bates & Jackson, 1987). The glass is thought to be a homogeneous non-crystalline material, but it is not completely homogeneous in its composition and texture due to internal impurities. The impurity comes from the very tiny micrometer-sized crystals, called microlites (Clark, 1961; Ross, 1962). Thus we can divide the internal structure of obsidian into microlites and glassy host matrix. In Korean obsidian artifacts there exist lots of microlites which were produced from quenching of acidic magma (Jin et al., 2014; Hwang & Jwa, 2017).

The microlite study is not a something new. It is well known that the microlite is crystallized phases under the supercooled condition of volcanic magma. Though a considerable amount of mineralogical study on microlites has been done since the 1960's (for example Clark, 1961; Ross, 1962; Donaldson, 1976, etc.), the researchers who tried to interpret the provenance of obsidian artifacts using geochemical data have overlooked the chemical effect of the microlites. Also, geochemical analyses for obsidian often show inconsistent results according to the technical methods. Suda et al. (2018) compiled and compared many analytical techniques used in the provenance study on the obsidian artifacts, and they found that the main discrepancy between the whole-rock and spot analyses comes from the existence of microphenocrysts (microlites) in the obsidian.

In this study, we first examined the morphology, texture, and composition of microlites in the two different obsidian source rocks. Then we investigated the compositional contrasts of the host matrix in the two obsidians. Finally, we attempted to evaluate the major discriminating factors between the two different sources – the Baekdusan obsidians and the Kyushu obsidians.

Figure 1. Major prehistoric obsidian localities in South Korea. Obsidian outcrops in Baekdusan and Kyushu are also indicated (Yi & Jwa, 2016).

2 Microlites in Obsidian

According to the morphological discrimination of microlites compiled by Clark (1961), the most abundant morphological features in the Baekdusan and Kyushu obsidians are trichites acicular and asteroidal, arculites, crenulites, ferculites, lath-crystals, scopulites and so on (Jin et al., 2014; Hwang & Jwa, 2017; Jwa & Hwang, in press), which are well observed under high magnification of the optical microscope. However, when we examine the microlites through high-resolution scanning electron microscope, they show very distinct mineral assemblage and/or texture (Hwang & Jwa, 2017; Jwa & Hwang, in press). For example, the microlites in the Baekdusan and Kyushu obsidians represent the different textural relationship. Early-crystallized Fe-oxides in the Baekdusan obsidians occur within the oikocrysts of clinopyroxene, showing poikilitic texture (Fig. 2). On the other hand, the clinopyroxene microlites in the Kyushu obsidians are overgrowing around the Fe-oxides or interlocking with the Fe-oxides (Fig. 2). This kind of texture between Fe-oxide and clinopyroxene would indicate the differing crystallization process of quenching rhyolitic magma (Befus, 2014).

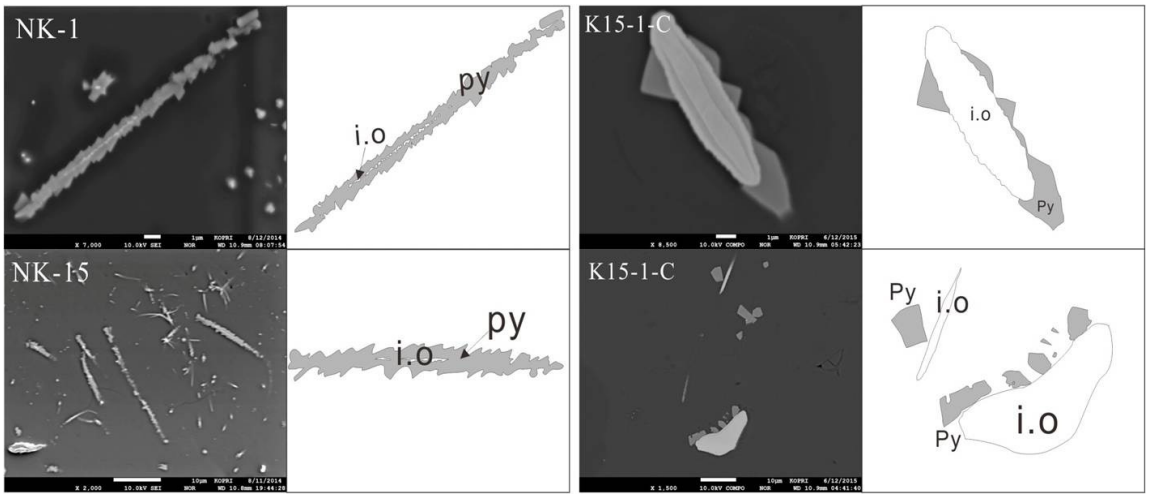

Figure 2. Secondary electron microscope (SEM) images and their sketches of the microlites in the Baekdusan (left) and Kyushu (right) obsidians. Hair-like microlites show poikilitic texture of Fe-oxides and clinopyroxenes in the Baekdusan obsidians, whereas clinopyroxenes occur as overgrowths on or intergrowths with clinopyroxenes in the Kyushu obsidians. Abbreviations: i.o, Fe-oxide; py, clinopyroxene.

Using the result of phase equilibrium experiments conducted by Befus (2014), we examined the crystallization sequence of the microlites at two different oxygen buffers. The buffers are oxygen fugacity approximately one log unit above the Ni-NiO oxygen buffer (NNO+1) and oxygen fugacity buffered at quartz-magnetite-fayalite buffer (QFM). The phase stabilities from both NNO+1 and QFM experiments are similar, if not identical, in the hydrostatic pressure range of 25 MPa to 150 MPa. Fe-oxides are of liquid phases, indicating that Fe-oxide microlites crystallize first from a quenching rhyolitic magma (Befus, 2014; Befus & Gardner, 2016). Sanidine (alkali feldspar) is the next phase to crystallize with decreasing temperature, and clinopyroxene stabilizes at a lower temperature than sanidine at equivalent pressure. Thus if the quenching magma starts to crystallize at slightly higher temperature than liquius, Fe-oxide and clinopyroxene crystallize in sequence, which is capable of explaining the poikilitic texture of Fe-oxide and clinopyroxene microlites in the Baekdusan obsidians. On the contrary, if the magma begins to crystallize at just below the liquidus, there occurs synchronous crystallization of Fe-oxide and clinopyroxene (Befus, 2014; Befus & Gardner, 2016), which are indicative of intergrowth and/or overgrowth texture of Fe-oxide and clinopyroxene microlites in the Kyushu obsidians. Consequently, the textural contrast of the Fe-oxide and clinopyroxene microlites in the Baekdusan and Kyushu obsidians suggests that the microlite crystallization in the Baekdusan obsidian started at a higher temperature of the magma.

Feldspar microlites appear mostly as a single lath-type grain or an aggregate of narrow prismatic grains. It is striking that the feldspar microlites in the Baekdusan obsidian are of alkali feldspar, whereas those in the Kyushu are of plagioclase. Considering that plagioclase is the final phase to stabilize in NNO+1 experiments but not in QFM experiments (Befus, 2014), the Baekdusan obsidians would have solidified under relatively low oxygen fugacity. On the other hand, alkali feldspar is known to be stable at relatively slower ascent rate (Befus, 2014). Lack of alkali feldspar microlites in the Kyushu obsidians indicates that the ascent (or decompression) rate of rhyolitic magma would have been relatively high. The most contrasting mineral assemblage between the Baekdusan and Kyushu obsidians is that crenulitic biotite microlites exclusively occur in the Kyushu obsidians. The occurrence of biotite microlites would indicate the H_2O-saturated phase relations in the Kyushu obsidians (Castro & Dingwell, 2009). From the mineral assemblage and texture of the microlites, it can be speculated that the two kinds of rhyolitic magmas which produced the Baekdusan and Kyushu obsidians, respectively, had solidified under different physical conditions such as oxygen fugacity, crystallization temperature, ascent rate, H_2O-saturation, and so on.

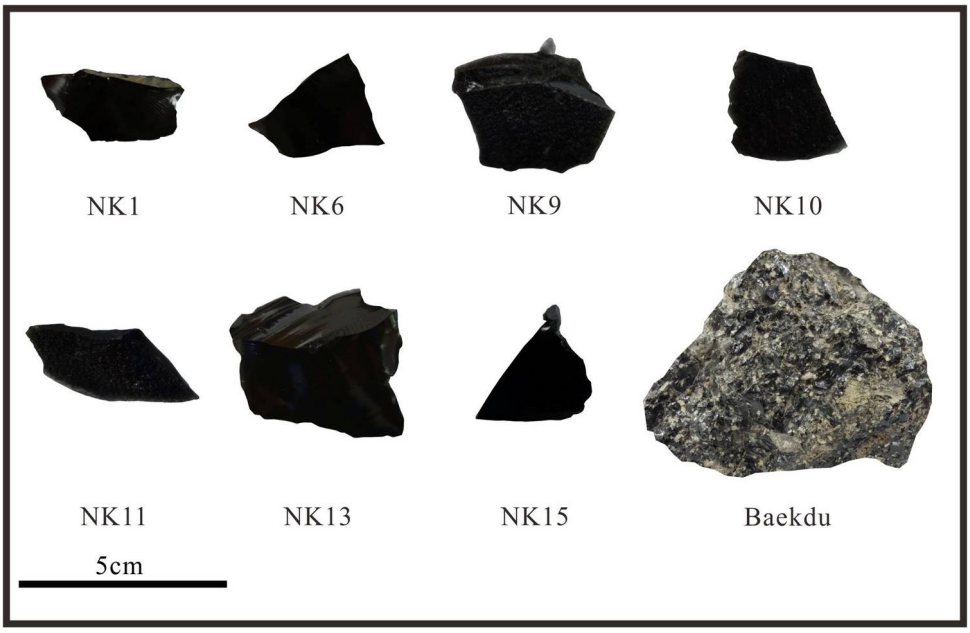

Figure 3. The Baekdusan obsidians used in this study. Seven NK obsidians were collected from a massive obsidian mine located at the southern flank of Mt. Baekdusan, and one sample, Baekdu, was from a trachytic lava layer.

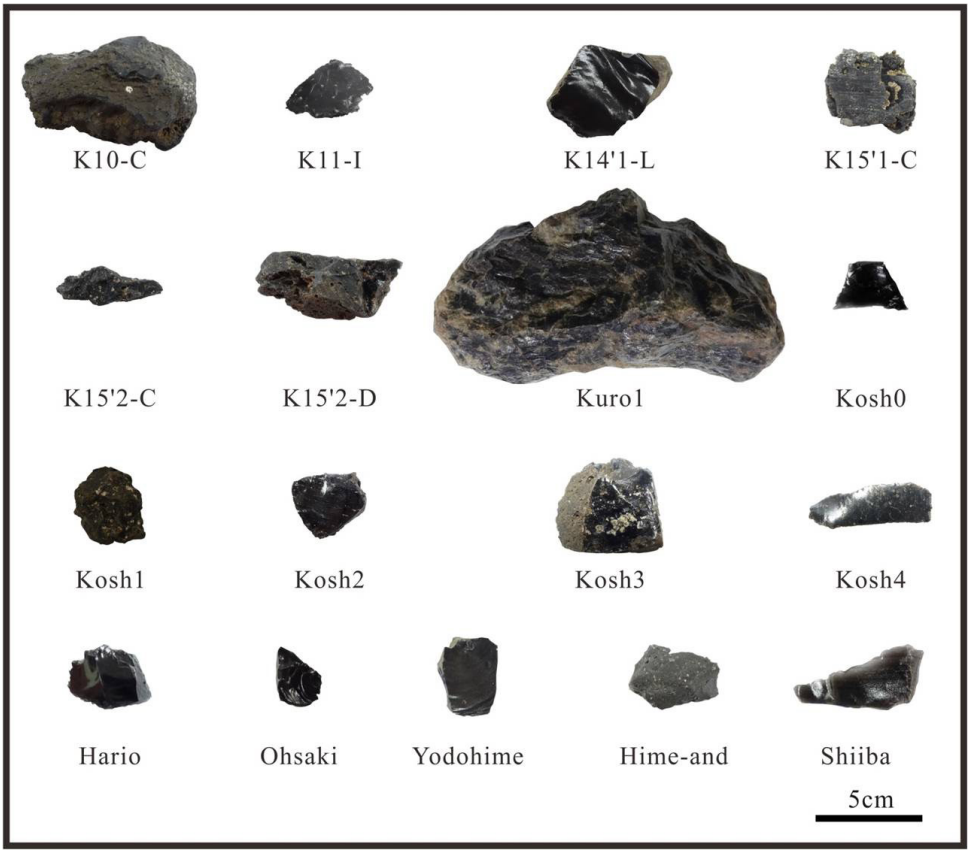

Figure 4. The Kyushu obsidians used in this study. The obsidian samples were collected from outcrops of seven localities: Koshidake (K10-C, K11-I, K14’1-L, K15’1-C, K15’2-C, K15’2-D, Kosh0, Kosh1, Kosh2, Kosh3, Kosh4), Kurogamiyama (Kuro 1), Hari-oshima (Hario), Ohsaki Peninsula (Ohsaki), Yodohime Higashihama (Yodohime), Himeshima (Hime-and), Shiibagawa (Shiiba).

3 Materials and Method

We collected natural obsidian samples both from the southern flank of the Baekdusan area and from the northern part of Kyushu of southwest Japan (Fig. 1). The Baekdusan and Kyushu obsidians used in this study are listed in Fig. 3 and Fig. 4, respectively. Since microlites are too small to analyze, we measured the major oxide composition of microlites using a field-emission-type electron microprobe (FE-EPMA) JEOL JXA-8530F with an acceleration voltage of 10 kV and beam current of 20 nA at the Korean Polar Research Institute. Microlites were analyzed with a focused beam of 1 μm diameter. Natural silicates were used as standards, and matrix corrections were calculated using a ZAF correction program. The detailed analytical procedure of FE-EPMA is described in Kim et al. (2018). Before analysis, the obsidian samples were photographed and imaged by field-emission-type scanning electron microscope (FE-SEM) JEOL JSM-7601F at the Gyeongsang National University. The analyzed chemical compositions of clinopyroxene and feldspar are listed in Tables 1 to 4.

Table 1. Chemical compositions (wt.%) of clinopyroxene microlites in the Baekdusan obsidians.

	Baekdu						NK1				NK11		NK15	
SiO2	48.6	48.4	48.5	48.5	47.5	47.0	41.6	44.1	43.1	43.5	42.3	47.9	48.6	42.7	40.5
TiO2	0.3	0.5	0.6	0.7	1.1	1.3	0.1	0.05	0.1	0.1	0.1	0.3	0.1	0.1	0.03
Al2O3	0.1	0.4	0.7	0.8	0.7	1.8	6.1	6.7	6.6	6.6	6.5	1.1	7.8	6.9	6.4
FeO	29.5	28.5	27.4	27.4	29.1	25.2	32.0	25.0	33.0	25.8	30.7	25.2	25.0	25.5	33.4
MnO	0.9	1.1	1.0	1.0	1.2	1.1	0.8	0.8	0.9	1.0	0.8	1.0	0.8	0.9	0.7
MgO	0.4	1.1	1.6	1.4	1.0	2.6	1.7	1.8	1.6	1.7	1.6	4.7	2.3	2.4	2.0
CaO	17.1	19.6	18.2	18.6	17.1	18.7	15.9	19.6	15.7	18.5	16.4	17.5	15.9	19.0	15.1
Na_2O	1.8	0.5	1.1	0.8	0.9	0.7	0.5	0.6	0.4	0.6	0.4	0.5	0.4	0.4	0.4
K_2O	-	-	0.2	0.1	0.1	0.2	0.2	0.2	0.3	0.2	0.2	0.1	0.3	0.2	0.2
Total	98.8	100.1	99.5	99.4	98.8	98.5	99.0	99.1	101.7	98.1	98.9	98.3	101.3	98.2	98.7
mol% of CaSiO3(Wo)-MgSiO3(En)-FeSiO3(Fs)															
Wo	42.1	45.2	43.5	44.4	41.4	44.6	36.7	47.1	35.9	45.0	38.5	40.1	41.2	45.0	34.4
En	1.3	3.5	5.5	4.6	3.4	8.5	5.6	6.1	5.1	5.9	5.3	14.8	8.4	7.8	6.3
Fs	56.6	51.2	51.0	51.0	55.2	46.9	57.7	46.8	59.1	49.0	56.2	45.1	50.5	47.2	59.3

Table 2. Chemical compositions (wt.%) of clinopyroxene microlites in the Kyushu obsidians

	Kosh0	Shiiba	Kuro1		Kosh1			K11-I		K14'1-L
SiO2	46.3	44.2	44.9	48.8	46.3	50.5	50.8	42.1	48.2	49.6	49.3
TiO2	0.01	1.0	0.1	0.1	0.04	0.02	0.07	0.04	0.09	0.08	0.21
Al2O3	7.1	15.7	5.9	8.4	5.8	7.0	7.0	5.7	1.0	1.4	1.9
FeO	36.2	21.0	38.0	36.1	36.8	34.5	33.5	43.3	36.6	37.0	34.9
MnO	2.2	0.1	2.4	1.3	2.3	2.0	1.7	1.9	1.9	2.1	1.8
MgO	7.0	7.3	2.7	3.3	5.7	4.7	4.4	5.2	9.4	8.0	8.6
CaO	1.0	0.1	4.3	0.9	1.5	1.5	1.6	1.4	1.8	1.7	2.1
Na_2O	0.07	1.18	0.28	0.51	0.24	0.52	0.78	0.23	0.04	0.12	0.11
K_2O	0.19	8.05	0.54	1.18	0.28	0.88	1.02	0.20	0.08	0.28	0.20
Total	100.2	98.7	99.0	100.7	99.0	101.5	100.9	100.1	99.1	100.3	99.0

continued **Table 2.** Chemical compositions (wt.%) of clinopyroxene microlites in the Kyushu obsidians

mol% of CaSiO3(Wo)-MgSiO3(En)-FeSiO3(Fs)											
Wo	2.6	0.3	11.4	2.7	3.9	4.4	4.6	3.4	4.2	4.0	5.0
En	25.0	38.2	9.8	13.7	20.9	18.5	18.2	17.1	30.1	26.7	29.0
Fs	72.4	61.5	78.8	83.6	75.2	77.1	77.2	79.5	65.7	69.2	66.1
					K15'1-C					**K15'2-C**	**K15'2-D**
SiO2	44.4	45.4	44.7	45.9	44.3	44.4	44.7	46.7	46.3	43.8	45.4
TiO2	0.05	0.00	0.00	0.11	0.00	0.07	0.02	0.03	0.10	0.00	0.01
Al2O3	6.1	5.6	6.8	3.9	6.2	7.7	6.1	3.8	3.9	6.7	5.0
FeO	36.7	37.2	36.5	36.4	37.5	37.4	37.3	38.3	36.8	37.5	36.8
MnO	2.4	2.3	2.2	2.4	2.5	2.3	2.5	2.7	2.6	2.7	2.4
MgO	7.7	7.0	6.8	8.3	6.7	7.0	6.7	7.0	8.4	6.0	7.8
CaO	1.3	1.0	1.2	0.8	1.2	1.0	1.2	0.9	1.2	1.4	1.5
Na2O	0.04	0.02	0.03	0.03	0.01	0.03	0.03	0.07	0.01	0.06	0.05
K2O	0.00	0.14	0.08	0.05	0.04	0.07	0.06	0.04	0.12	0.03	0.01
Total	98.7	98.6	98.3	98.0	98.4	99.9	98.6	99.5	99.5	98.1	98.9
mol% of CaSiO3(Wo)-MgSiO3(En)-FeSiO3(Fs)											
Wo	3.3	2.4	3.1	2.1	2.9	2.5	2.9	2.3	2.8	3.5	3.7
En	26.3	24.6	24.0	28.3	23.6	24.3	23.4	24.1	28.1	21.4	26.4
Fs	70.4	73.0	72.8	69.6	73.5	73.2	73.6	73.6	69.1	75.1	69.8

Table 3. Chemical compositions (wt.%) of feldspar microlites in the Baekdusan obsidians.

			Baekdu		
SiO2	67.7	69.7	68.2	67.6	67.8
TiO2	-	0.01	-	-	-
Al2O3	18.9	17.9	18.5	18.4	18.6
FeO	0.4	1.4	0.8	0.6	0.6
MnO	-	0.02	-	-	-
MgO	-	-	0.01	-	0.03
CaO	0.09	0.02	0.10	-	0.02
Na2O	7.0	5.9	6.7	7.4	7.3
K2O	7.1	5.6	6.9	6.4	6.8
Total	101.2	100.6	101.3	100.4	101.2
mol% of NaAlSi3O8(Ab)-CaAl2Si2O8(An)-KAlSi3O8(Or)					
Ab	59.5	61.2	59.5	63.8	62.0
An	0.4	0.1	0.5	0.0	0.1
Or	40.1	38.7	40.1	36.2	38.0

Table 4. Chemical compositions (wt.%) of feldspar microlites in the Kyushu obsidians.

	Shiiba					K10C			K11-I			K14'1-L				
SiO2	66.0	63.4	63.6	64.8	66.8	64.8	68.0	65.1	64.7	64.7	63.6	64.8	66.1	65.9	64.6	64.7
TiO2	0.05	0.00	-	0.03	0.03	-	-	0.01	0.04	0.03	-	-	-	0.03	-	0.03
Al2O3	22.0	23.1	22.9	23.2	21.5	22.4	21.6	21.9	23.1	23.1	22.7	22.1	22.0	22.0	22.7	22.2
FeO	0.1	0.1	0.0	0.1	0.3	0.3	0.2	0.1		0.3	0.3	0.2	0.4	0.2	0.4	0.3
MnO	-	0.01	0.01	0.09	-	0.06	0.08	-	0.01	0.01	0.12	-	0.08	-	-	0.07
MgO	-	-	-	-	0.04	0.00	0.01	-	0.002	-	0.03	-	-	0.02	0.02	0.03
CaO	3.7	4.9	4.7	4.8	4.1	3.5	2.5	2.8	3.9	3.8	4.2	3.4	3.1	2.6	3.6	3.5
Na2O	6.0	7.9	7.7	7.8	7.6	8.5	6.5	8.8	8.6	8.6	8.4	8.7	7.2	8.8	8.8	8.6
K2O	0.7	0.7	0.5	0.6	0.9	1.5	1.2	1.5	0.8	0.6	0.7	1.2	0.7	0.8	0.7	1.1
Total	98.6	100.2	99.6	101.4	101.3	101.1	100.2	100.4	101.5	101.1	100.1	100.3	99.7	100.4	100.8	100.6
mol% of NaAlSi3O8(Ab)-CaAl2Si2O8(An)-KAlSi3O8(Or)																
Ab	70.4	71.5	72.3	71.9	72.7	74.3	75.0	77.5	76.1	77.5	75.1	76.5	76.8	81.6	78.2	76.2
An	24.1	24.5	24.5	24.4	21.6	17.0	15.9	13.7	19.0	19.1	20.9	16.5	18.3	13.3	17.8	17.4
Or	5.5	4.0	3.2	3.7	5.7	8.7	9.1	8.7	4.8	3.4	4.0	7.0	5.0	5.1	4.1	6.4

For major oxide composition of the glassy matrix in obsidian, we conducted the wavelength dispersive (WDS) analysis using an electron microprobe JEOL JXA-8100 with an acceleration voltage of 15 kV, beam current of 10 nA at the Gyeongsang National University. To minimize Na migration during glass analyses we used a 10 μm diameter defocused beam. For the analysis of trace and rare earth element composition, we used LA-ICP-MS method at Korea Basic Science Institute. The detailed analytical procedure of LA-ICP-MS method is described in Yi & Jwa (2016). Analytical results for glassy host matrix are listed in Table 5.

4 Chemical Composition of Microlites

From the observation for the microlites in the Baekdusan and Kyushu obsidians, it is obvious that the textural relationship between clinopyroxenes and Fe oxides is different with respect to their source, which reflects the differing condition of undercooling in rhyolitic magmas (Hibbard, 1995; Befus, 2014). We analyzed clinopyroxene and feldspar microlites and compared their compositions concerning their sources (Fig. 5, Fig. 6).

From the $CaSiO_3$(Wo)-$MgSiO_3$(En)-$FeSiO_3$(Fs) discrimination, the clinopyroxene microlites from the Baekdusan obsidians have the composition of hedenbergite and augite ($Ws_{24\sim47}En_{1\sim15}Fs_{47\sim59}$), i.e., relatively Ca-rich but Mg- and Fe-poor. This kind of clinopyroxene composition is also recognized from the volcanic glass from Changbaishan (Chinese name for Baekdusan) Millennium eruption (Sun et al., 2016). On the other hand, the Kyushu obsidians have the composition of clinoferrosilite ($Ws_{0\sim11}En_{10\sim30}Fs_{61\sim80}$), that is relatively Fe- and Mg-rich, Ca-deficient. Thus the chemical composition of clinopyroxene is a good discriminator between the Baekdusan and Kyushu obsidians.

Feldspar microlites are the other discriminator between the two obsidians. Alkali feldspar appears to have formed readily in the Baekdusan obsidian but is lack in the Kyushu obsidian. Plagioclase is a predominant feldspar phase in the Kyushu obsidians, but it is not found in the Baekdusan obsidians. The occurrence of feldspar in both obsidians is well confirmed from the chemical composition of feldspar microlites (Fig. 6). From $KAlSi_3O_8$(Or)-$NaAlSi_3O_8$(Ab)-$CaAl_2Si_2O_8$(An) discrimination, the feldspar microlites from the Baekdusan obsidian show the composition of sanidine to anorthoclase ($Or_{36\sim40}Ab_{0\sim0.5}An_{36\sim40}$, alkali feldspar solid solution), indicating very low Ca but relatively high K contents. High Na contents in the

Table 5. Chemical compositions of the host matrix in the Baekdusan and Kyushu obsidians (major oxides in wt.%, trace and rare earth elements in ppm).

	Baekdusan obsidian								Kyushu obsidian								
	NK1	NK6	NK9	NK10	NK11	NK13	NK15	Baekdu	Hario	Ohsaki	Yodohime	Hime	Shiiba	Kosh1	Kosh2	Kosh3	Kosh4
SiO2	75.2	74.6	74.7	73.9	74.6	74.6	75.2	67.1	76.5	77.6	77.3	76.5	75.1	76.2	77.1	77.1	77.3
Al2O3	13.3	13.2	13.3	13.2	13.2	13.1	13.3	18.3	12.8	12.7	12.8	14.5	13.2	13.3	13.1	13.1	13.1
TiO2	0.08	0.07	0.11	0.10	0.07	0.06	0.09	0.07	0.06	0.08	0.02	0.02	0.06	0.07	0.03	0.05	0.03
FeO	0.63	1.13	1.25	1.23	1.26	1.25	0.62	0.83	0.72	0.33	0.59	0.90	0.98	0.84	0.71	0.72	0.44
MnO	0.02	0.04	0.03	0.05	0.05	0.05	0.02	0.03	0.04	0.03	0.05	0.11	0.05	0.04	0.04	0.07	0.02
MgO	0.00	0.02	0.03	0.02	0.02	0.00	0.01	0.02	0.03	-	0.01	0.06	0.13	0.05	0.03	0.04	0.03
Na2O	3.8	3.9	3.8	3.6	3.6	3.8	3.9	7.1	0.63	0.40	0.46	0.49	0.97	0.81	0.60	0.59	0.65
CaO	0.22	0.41	0.52	0.50	0.51	0.38	0.23	0.16	3.7	3.9	3.7	3.4	3.5	4.0	3.7	3.9	3.9
K2O	5.04	4.90	4.87	4.97	5.00	4.76	5.17	6.71	4.4	4.6	4.8	3.9	4.1	4.2	4.4	4.6	4.4
P2O5	0.03	0.03	0.03	0.03	0.01	0.01	0.02	0.04	0.03	0.04	0.02	0.07	0.04	0.04	0.03		0.01
Rb	239.6	255.4	189.3	223.5	229.5	216.9	205.7	363.7	196.6	202.4	127.0	85.1	176.3	218.8	175.8	176.4	187.1
Sr	10.1	10.6	10.9	13.6	13.6	8.8	10.7	0.4	38.0	26.3	95.8	43.4	158.9	39.4	38.1	34.1	40.4
Y	45.5	47.0	37.6	47.6	51.7	39.8	38.5	154.0	24.0	28.5	15.3	9.4	13.8	24.4	21.4	20.0	21.3
Zr	191.5	196.3	173.3	208.9	219.7	167.3	167.1	2444.0	62.5	113.7	112.2	20.0	76.9	69.8	61.6	57.0	59.3
Nb	93.7	99.1	81.4	89.4	91.1	83.2	79.9	295.0	20.8	19.7	18.7	17.4	23.2	21.1	18.3	16.6	18.4
Ba	42.8	43.9	47.5	58.3	55.2	36.8	45.8	0.8	214.6	377.4	525.6	732.4	728.1	250.2	216.2	204.2	223.7
La	57.0	58.8	47.5	59.2	61.7	49.3	48.4	270.2	22.6	36.3	33.6	6.1	34.2	26.2	22.9	20.5	23.6
Ce	130.4	135.7	104.1	125.8	127.0	112.7	109.6	539.5	44.5	69.0	59.9	15.4	61.5	48.5	43.3	38.2	44.3
Pr	12.7	13.3	10.1	12.9	13.3	11.0	10.9	55.0	4.2	6.9	5.4	1.8	5.5	4.7	4.1	3.7	4.1
Nd	44.1	46.6	36.3	46.6	48.1	39.0	38.2	199.8	14.0	24.2	17.7	6.8	18.4	15.0	13.0	12.6	13.1
Sm	9.2	9.9	7.3	9.7	10.0	7.8	8.0	38.5	3.3	4.7	3.2	2.2	3.3	3.4	3.0	2.7	2.8
Eu	0.2	0.2	0.2	0.2	0.2	0.2	0.2	0.6	0.2	0.2	0.4	0.1	0.4	0.2	0.2	0.2	0.2
Gd	8.6	8.6	6.6	8.7	9.2	7.4	7.1	34.4	3.3	4.4	2.6	2.1	2.7	3.6	3.3	2.9	3.0
Tb	1.3	1.4	1.0	1.4	1.5	1.1	1.1	5.1	0.6	0.7	0.4	0.3	0.4	0.7	0.6	0.5	0.6
Dy	8.7	8.9	6.6	8.9	9.3	7.4	7.3	31.7	4.1	4.8	2.7	1.7	2.3	4.4	3.9	3.4	3.7
Ho	1.6	1.7	1.3	1.7	1.8	1.4	1.4	6.0	0.8	0.9	0.5	0.3	0.4	0.9	0.8	0.7	0.8
Er	4.3	4.6	3.5	4.6	4.9	3.8	3.7	15.8	2.3	3.1	1.5	0.7	1.3	2.4	2.2	2.1	2.1
Tm	0.6	0.7	0.5	0.7	0.7	0.5	0.6	2.3	0.3	0.5	0.2	0.1	0.2	0.4	0.4	0.3	0.4
Yb	4.2	4.3	3.3	4.2	4.5	3.6	3.6	13.9	2.5	3.3	1.7	0.5	1.3	2.7	2.5	2.3	2.4
Lu	0.6	0.6	0.4	0.6	0.7	0.5	0.5	2.0	0.4	0.5	0.3	0.1	0.2	0.4	0.3	0.3	0.3
Hf	8.1	8.3	6.7	8.2	8.8	6.8	6.7	59.3	2.8	4.6	3.6	1.4	3.0	3.1	2.8	2.5	2.7
Ta	7.1	7.4	6.4	7.2	7.3	6.4	6.2	19.2	2.8	2.1	1.8	1.8	2.8	2.8	2.4	2.2	2.3

feldspar microlites from the Kyushu obsidian is characteristic and the feldspar is discriminated to oligoclase ($Or_{3\sim9}Ab_{70\sim82}An_{13\sim25}$, plagioclase solid solution).

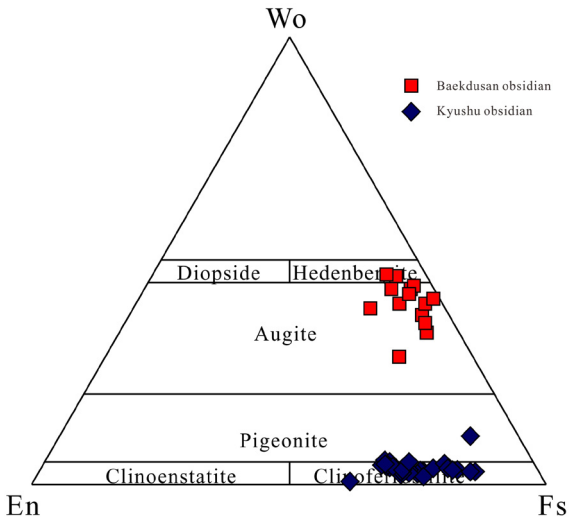

Figure 5. $CaSiO_3$(Wo) -$MgSiO_3$(En)-$FeSiO_3$(Fs) discrimination of clinopyroxene.

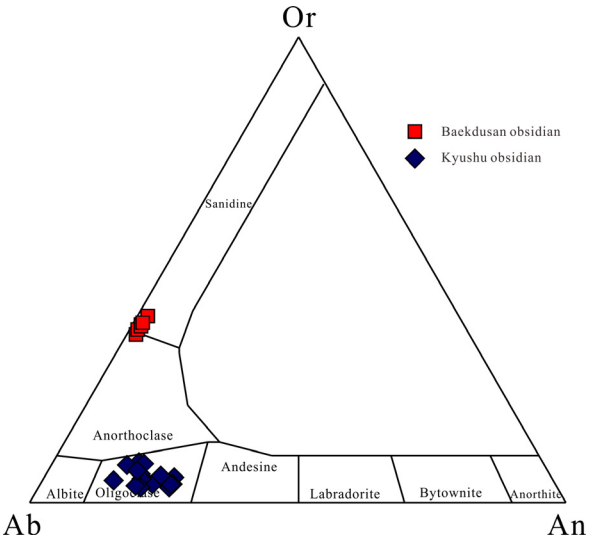

Figure 6. $KAlSi_3O_8$(Or)-$NaAlSi_3O_8$(Ab)-$CaAl_2Si_2O_8$(An) discrimination of feldspar.

5 Chemical Composition of Glassy Matrix

We acquired the major oxide, trace and rare earth element compositions for the glassy host matrix. In general, the matrix composition of volcanic rocks represents the chemical composition of liquid at a solidifying temperature. By comparing the matrix compositions between the two obsidians, we examined the chemical contrast of two rhyolitic magmas which produced obsidians.

In Fig. 7 we can see that the major oxide contents in the Baekdusan and Kyushu obsidians are systematically decreased or increased with SiO_2, but the variation trend of each obsidian is quite different. At the SiO_2 range of 74 to 78 wt.%, the host glasses of the Baekdusan obsidians have higher contents of TiO_2, FeOT (total Fe as FeO), Na_2O, K_2O than those of the Kyushu obsidians. It is striking that the alkaline contents

of the Baekdusan obsidians are high but CaO contents are very low. Similarly, there exists compositional contrast between the two obsidians in the variation of trace element contents (Fig. 8). At the SiO_2 range of 74 to 78 wt.%, the host glasses of the Baekdusan obsidians have higher contents of Y and high field-strength elements (HFSEs, small radius but high charge ions) such as Nb, Hf, Zr, Ta than those of the Kyushu obsidians.

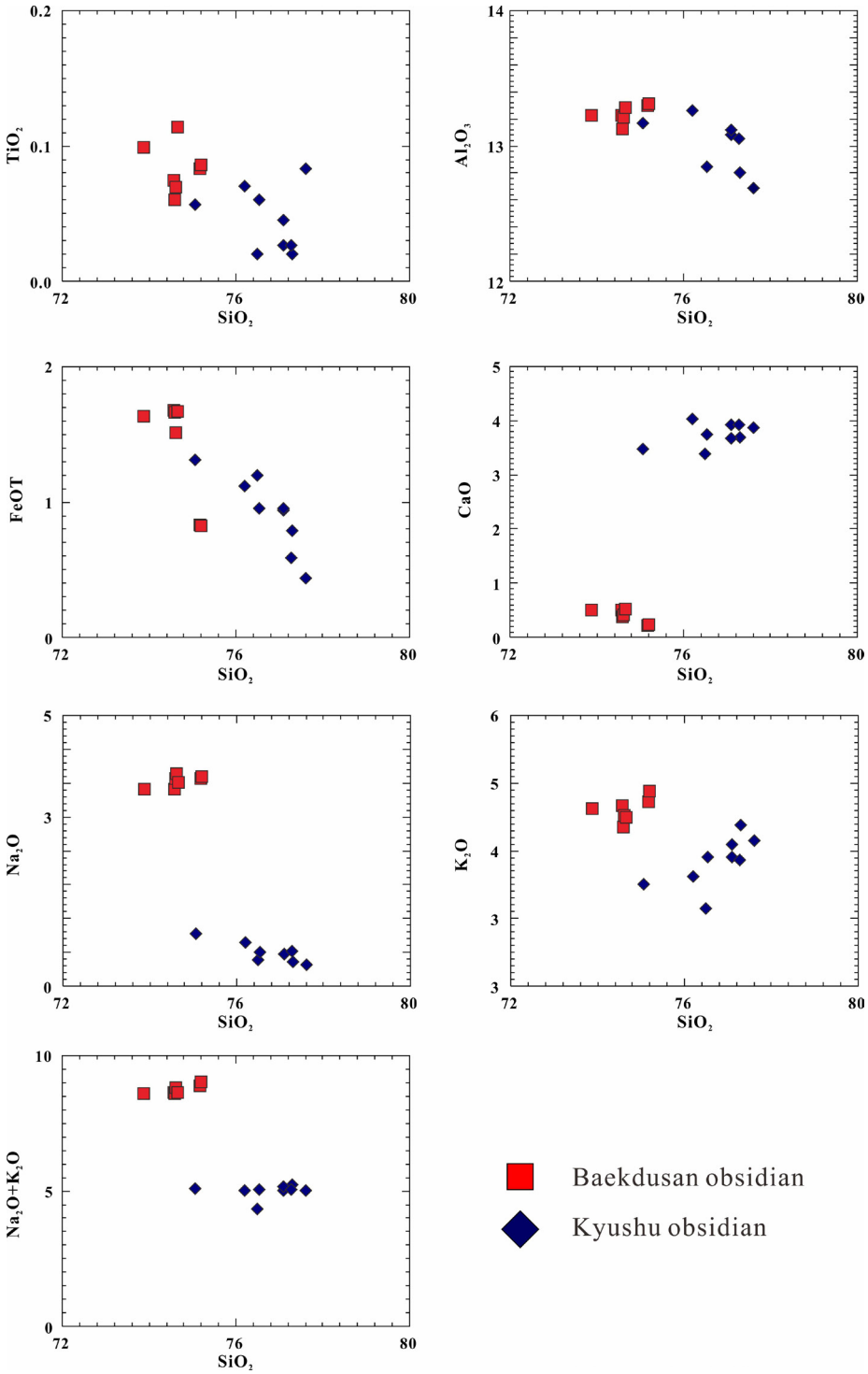

Figure 7. SiO_2 versus major oxide contents (wt. %) variation diagrams for the Baekdusan and Kyushu obsidians.

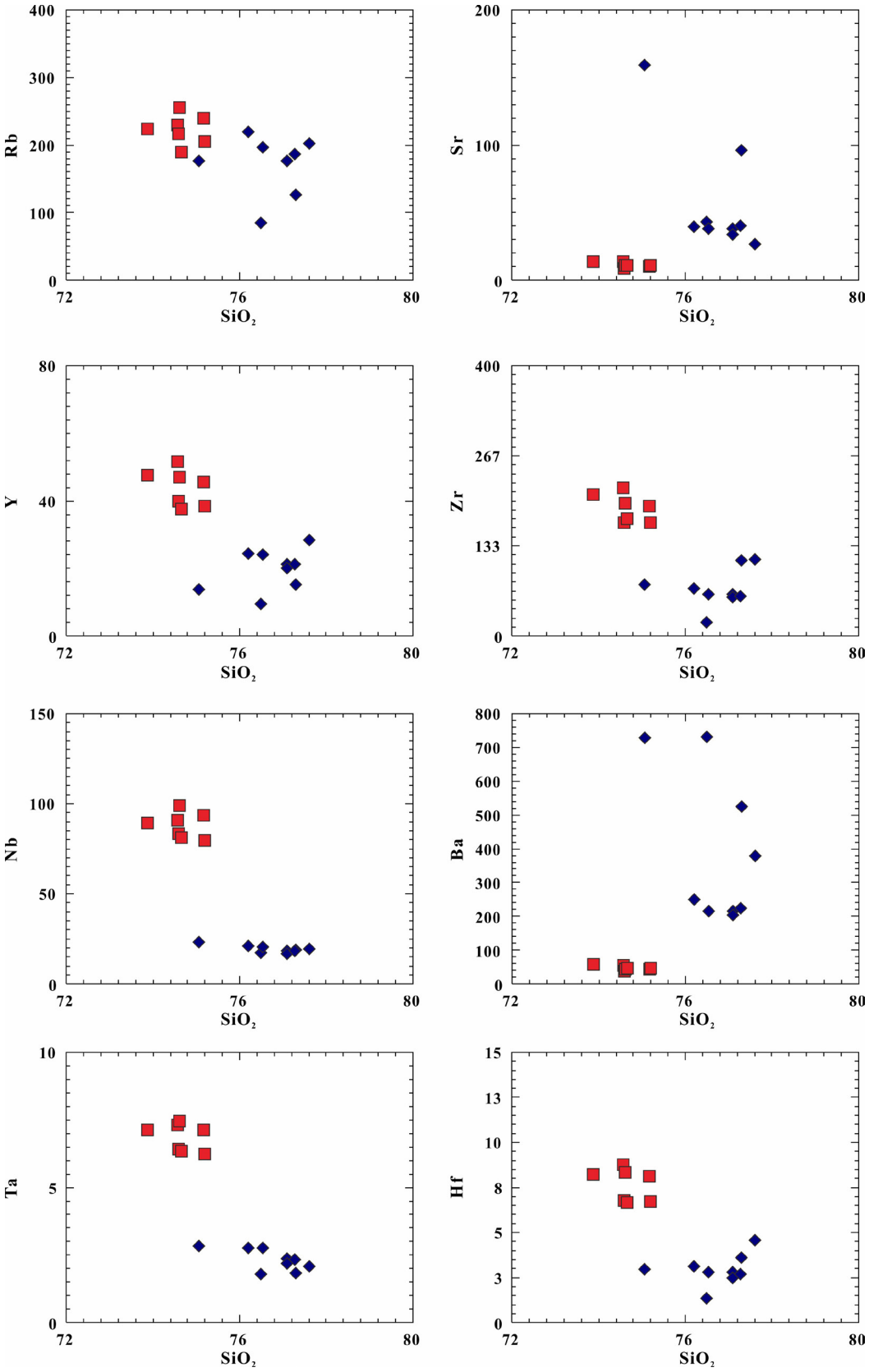

Figure 8. SiO_2 (wt.%) versus trace element contents (ppm) variation diagrams for the Baekdusan and Kyushu obsidians. The symbols are the same as Fig. 7.

We compared the rare earth elements compositions of the two obsidians using REE pattern (Fig. 9), which would be a very effective indicator to investigate the petrologic relationship among the rocks (Henderson, 1984). The REE pattern is deduced from the relative REE composition of samples to the certain standard materials such as chondrite, mid-oceanic ridge basalt, continental crust, etc. Here, we use the chondrite-normalized REE pattern. If two rocks under comparison are genetically correlated with each other, their REE patterns should be similar; that is, the pattern shape and the relative composition should be nearly the same. Excluding anomalous lower trough of Eu, the entire REE patterns of the Baekdusan obsidians are higher than those of the Kyushu obsidians (Fig. 9), which indicates that the total REE contents are higher in the Baekdusan obsidians. The negative anomaly of Eu in the REE pattern suggests feldspar fractionation during magmatic evolution (Henderson, 1984). Strong negative Eu anomaly for the Baekdusan obsidians is indicative of strong feldspar fractionation of rhyolitic magma in the Baekdusan volcanic field.

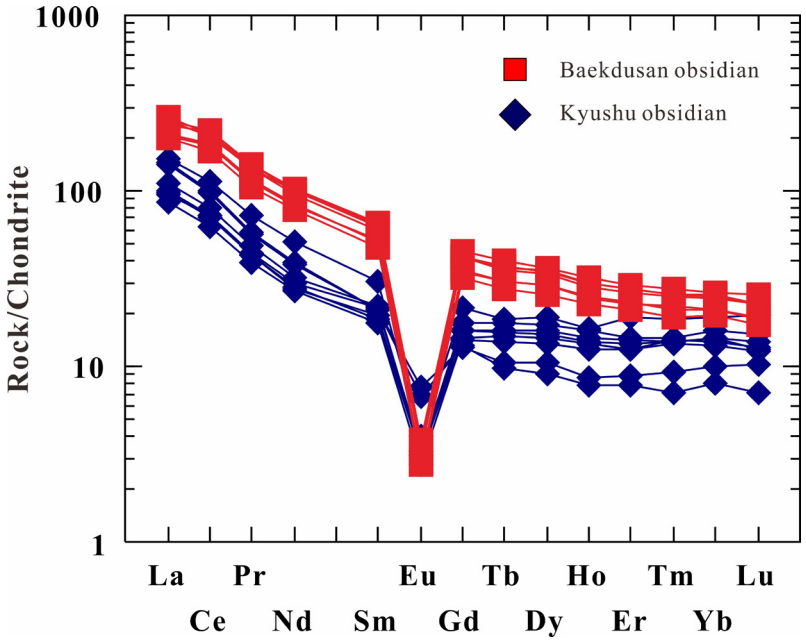

Figure 9. Chondrite-normalized rare earth elements (REEs) patterns for the Baekdusan and Kyushu obsidians.

The chemical contrast between the Baekdusan and Kyushu obsidians would have come from the different parental magma genesis. The Baekdusan and the Kyushu volcanic fields are geologically different in the tectonic environment. Baekdusan volcanism occurred within the anorogenic continental environment, whereas Kyushu volcanism is the product of the active subduction zone magmatism (Zou et al., 2008; Zhao & Liu, 2010). This environmental contrast resulted in the different geochemical characteristics of the volcanic magma, essentially leading to the different chemical composition of the obsidians. Yi & Jwa (2016) investigated the tectonic contrast between the two areas using Pb isotopic composition of obsidian, and found that the Baekdusan obsidians have higher isotopic ratios of $^{208}Pb/^{204}Pb$ and $^{207}Pb/^{204}Pb$ at a given $^{206}Pb/^{204}Pb$ ratio, indicating that the crustal components were highly engaged in generating volcanic magma. On the other hand, the Kyushu volcanic rocks have lower Pb isotopic ratios which are indicative of the relative contribution of mantle component to the volcanic magma.

Considering that the Baekdusan is situated in different tectonic setting from Kyushu, the resultant geochemical contrast would have been originated from the different magma genesis and differentiation process. This fact would be a useful discriminator in isolating and identifying the obsidian provenances.

Table 6. Mineralogical and geochemical characteristics of the Baekdusan and Kyushu obsidians.

Characteristics	Baekdusan obsidians	Kyushu obsidians	Reference
Microlite morphology	acicular, asteroidal, cumulite	acicular, margarite, lath, asteroidal, crenulite	Hwang & Jwa (2017)
Mineral assemblage	Fe-oxide, clinopyroxene, alkali feldspar	Fe-oxide, clinopyroxene, plagioclase, biotite	Hwang & Jwa (2017)
Microlite texture	Fe-oxide within clinopyroxene (poikilitic)	clinopyroxene overgrowth on Fe-oxide	Hwang & Jwa (2017)
Clinopyroxene composition	augite~hedenbergite	ferrosilite	This study
Feldspar composition	sanidine~anorthoclase	oligoclase	This study
Major oxide content	higher total FeO & Na_2O+K_2O lower CaO	lower total FeO & Na_2O+K_2O higher CaO	This study
Trace element content	higher Y, Zr, Nb, Hf, Ta lower Sr	lower Y, Zr, Nb, Hf, Ta higher Sr	This study
REE content and pattern	higher REE contents strong Eu negative anomaly	lower REE contents moderate Eu negative anomaly	This study
Pb isotopic ratio	higher $^{207}Pb/^{204}Pb$ & $^{208}Pb/^{204}Pb$ ratios	lower $^{207}Pb/^{204}Pb$ & $^{208}Pb/^{204}Pb$ ratios	Yi & Jwa (2016)
Tectonic environment	within-plate	volcanic-arc	Yi & Jwa (2016)

6 Concluding Remarks

We compared the Baekdusan and Kyushu obsidians regarding microlite morphology and texture, microlite chemistry and geochemical characteristics of glassy host matrix and so on. Such a comparison shows that there are distinctive mineralogical and geochemical characteristics of the two obsidians, which is likely to have been controlled by the crystallization process and initial composition of rhyolitic magmas under the different tectonic environment. We summarized significant contrasts between the Baekdusan and Kyushu obsidians in Table 6. Clinopyroxene and feldspar compositions are decisive to determine where the obsidian was originated. Higher contents of alkaline and high field strength elements in the host matrix are characteristic in the Baekdusan obsidians, whereas higher CaO and Sr contents are evident in the Kyushu obsidians. Higher REE contents and strong Eu negative anomaly are indicative of the Baekdusan obsidians. Thus these features would be a useful discriminator to divide the two obsidians from the Baekdusan and the Kyushu volcanic field.

Furthermore, the mineralogical and geochemical consideration can discriminate the sources of the obsidian artifacts in South Korea. Also, the overall geochemical dataset for the Baekdusan and Kyushu obsidians can be used to interpret the provenance of the obsidian artifacts from the prehistoric sites in the Korean Peninsula as well as contiguous areas such as China, Japan, and Russia.

Acknowledgments: This work was supported by the National Research Foundation of Korea (NRF) Grant funded by the Korea government (MSIP) (NRF-2012M2A2A6004263). This paper has benefitted from reviews by two anonymous reviewers.

References

Bates, R.L. & Jackson, J.A. (1987). *Glossary of Geology*. Alexandria, Virginia: American Geological Institute.

Befus, K.S. (2014). *Storage, ascent, and emplacement of rhyolite lavas* (unpublished doctoral dissertation). The University of Texas, Austin.

Befus, K.S. & Gardner, J.E. (2016). Magma storage and evolution of the most recent effusive and explosive eruptions from Yellowstone Caldera. *Contributions to Mineralogy and Petrology*, 171: 30. Retrieved from https://link.springer.com/article/10.1007/s00410-016-1244-x.

Castro, J.M. & Dingwell, D.B. (2009). Rapid ascent of rhyolitic magma at Chaiten volcano, Chile. *Nature*, 461:8. doi:10.1038/nature08459.

Chang, Y. & Kim, J.C. (2018). Provenance of obsidian artifacts from the Wolseongdong Paleolithic site, Korea, and its archaeological implications. *Quaternary International*, 467, 360–368.

Cho, N.-C. & Choi, S.-Y. (2010). Provenance study of obsidian from Gigok paleolithic site in Donghae-si using trace elements. *Journal of Korean Ancient Historical Society*, 70, 5–20. (Korean with English abstract)

Cho, N.-C. & Choi, S.-Y. (2012). Chemical composition and provenance study of obsidian from Sangsa-ri Paleolithic site in Cheolwon. *Journal of Korean Ancient Historical Society*, 78, 5–21. (Korean with English abstract)

Cho, N.-C., Kang, H.-T., & Chung, K.-Y. (2006). Provenance study of obsidian artifacts found in the Korean peninsula based on trace elements and Sr isotope ratios. *Journal of Korean Ancient Historical Society*, 53, 5–21. (Korean with English abstract)

Clark, D.L. (1961). *The application of the obsidian dating method to the archaeology of central California* (unpublished doctoral dissertation). Stanford University.

Donaldson, C.H. (1976). An experimental investigation of olivine morphology. *Contributions to Mineralogy and Petrology*, 57, 187–213.

Henderson, P. (1984). *Rare earth element geochemistry*. Amsterdam: Elsevier.

Hibbard, M.J. (1995). *Petrography to petrogenesis*. New Jersey: Prentice-Hall.

Hwang. G.-H. & Jwa, Y.-J. (2017). Morphology and texture of microlites in the Baekdusan and Kyushu obsidians. *Journal of Korean Earth Science Society*, 38, 546–551. (in Korean with English summary)

Jang, Y.D., Park, T.Y., Lee, S.M., Kim, J.J. (2007). Petrologic and mineralogic studies on the origin of Paleolithic obsidian implements from Wolseong-dong, *Korea*. *Journal of Korean Earth Science Society*, 28, 731–740. (Korean with English abstract)

Jin, M.E., Moon, S.W., Ryu, C.K., Jwa, Y.-J. (2014). Mineralogical study on microlites in the Baekdusan obsidian and the Gadeokdo obsidian artefacts. *Journal of Mineralogical Society of Korea*, 27, 243–249. (in Korean with English summary)

Jwa, Y.-J. & Hwang, G.-H. (in press). Detailed morphology and texture of microlites in obsidian observed through electron microscopy. *Journal of Korean Earth Science Society.* (Korean with English summary)

Kim, J.C., Kim, D.K., Youn, M., Yun, C.C., Park, G., Woo, H.J., Hong, M.-Y., Lee, G.K. (2007). PIXE provenancing obsidian artifacts from Paleolithic sites in Korea. *Indo-Pacific Prehistory Assoc. Bulletin*, 27, 122–128.

Kim. D., Kim, T., Lee, J., Kim, Y., Kim, H., Lee, J.Ik. (2018). Microfabrics of omphacite and garnet in eclogite from the Laterman Range, northern Victoria Land, Antarctica. *Geosciences Journal,* 22, 939–953.

Kuzmin, Y.V. (2004). *Obsidian compositional analysis for Paleo-/Mesolithic Hongcheon Hahwagye-ri site*. Gangwon Archaeological Institute. (in Korean)

Lee, G.K. & Kim, J.C. (2015). Obsidians from the Sinbuk archaeological site in Korea - Evidences for strait crossing and long-distance exchange of raw material in Paleolithic Age. *Journal of Archaeological Science: Reports*, 2, 458–466.

Sohn, P.K. (1989). *Provenance of obsidian found in Sangmuryong-ri*. Gangwon National University Museum, 781–796. (in Korean)

Suda, Y., Grebennikov, A.V., Kuzmin, Y., Glasscock, M.D., Wada, K., Ferguson, J.R., Kim, J.C., Popov, V.K., Rasskazov, S.V., Yasnygina, T.A., Saito, N., Takehara, H., Carter, T., Kaszovszky, Z., Biro, K.T., Ono, A. (2018). Inter-laboratory validation of the WDXRF, EDXRF, ICP-MS, NAA and PGAA analytical techniques and geochemical charaterisation of obsidian sources in northeast Hokkaido Island, Japan. *Journal of Archaeological Science: Reports*, 17, 379–392.

Sun, C.Q. (2016). Clinopyroxene and Fe-Ti oxides for correlating the ash from Changbaishan Millenium eruption. Science China: *Earth Sciences*, 59, 1454–1462.

Yi, S. & Jwa, Y.-J. (2016). On the provenance of prehistoric obsidian artifacts in South Korea. *Quaternary International*, 392, 37–43

Zhao, D. & Liu, L. (2010). Deep structure and origin of active volcanoes in China. *Geoscience Frontiers*, 1, 31–44.

Zou, H., Fan, Q., & Yao, Y. (2008). U-Th systematics of dispersed young volcanoes in NE China: Asthenosphere upwelling caused by piling up and upward thickening of stagnant Pacific slab. *Chemical Geology*, 255, 134–142.